

# JOURNAL OF THE STRUCTURAL DIVISION

## CONCRETE REINFORCING NET: OPTIMUM SLIP-FREE LIMIT DESIGN

By Zdeněk P. Bažant,<sup>1</sup> M. ASCE and Tatsuya Tsubaki<sup>2</sup>

### DESIGN PHILOSOPHY

Design of regular reinforcing nets is a fundamental problem for concrete shells, slabs, shear walls, box girders and vessels, prestressed as well as unprestressed, and has been studied intensively (1,2,6-8,10,14,15,23,24). Excluding from this study the problem of internal force redistribution within the structure as a whole, which is hard to treat analytically, and assuming that the internal forces are known or have been at least approximately determined, we face the problem of finding the necessary cross-sectional areas of reinforcement and eventually also the thickness of concrete. For this task, basically two design concepts are being used: (a) The design based on limit capacity of reinforcement; and (b) the design based on service stresses.

In the current limit capacity concept, steel bars are assumed to yield and concrete is assumed to provide resistance only to the compression force parallel to a crack. Only equilibrium conditions are used and equilibrium under the ultimate load must be satisfied for all possible crack directions (1,2,10). The current limit analysis concept for reinforcing nets can be traced back to Leitz (15). A particularly systematic and comprehensive coverage was given by Baumann (1). The limit capacity concept is implied by Articles 9.2, 9.3, and 19.5 of American Concrete Institute (ACI) Standard 318 (3) and Articles 19.3.2 and 19.3.3 of ACI Standard 349 (5), although, as has been pointed out by Gupta (10), the present terse wording of these articles could be misinterpreted to mean that satisfying equilibrium for only two directions is sufficient. This would be incorrect because the upper bound theorem of limit analysis states that the true failure mode (in our case, the true crack direction) is that for which the failure load is smallest, and so fulfillment of equilibrium on a crack of *any* direction is essential. Apart from this argument, it must be also noted that,

Note.—Discussion open until July 1, 1979. To extend the closing date one month, a written request must be filed with the Editor of Technical Publications, ASCE. This paper is part of the copyrighted Journal of the Structural Division, Proceedings of the American Society of Civil Engineers, Vol. 105, No. ST1, February, 1979. Manuscript was submitted for review for possible publication on May 24, 1978.

<sup>1</sup>Prof. of Civ. Engrg., Northwestern Univ., Evanston, Ill.

<sup>2</sup>Grad. Research Asst., Northwestern Univ., Evanston, Ill.

in nonprestressed concrete, shrinkage and temperature stresses as well as previous loads may produce a crack of any direction, existing before the ultimate load is introduced.

In the current service stress concept (6), the steel bars in tension, as well as concrete under compression parallel to the crack, are considered to be elastic, limited to allowable stresses. The critical crack direction is found from the conditions of compatibility of the strains in steel and concrete, which leads to a nonlinear (transcendental) equation for the crack angle.

The service stress concept is preferable for nuclear reactor containments (1), for it assures the strains in steel bars under service conditions to be small, which in turn prevents the occurrence of wider tensile cracks in concrete. The limit capacity concept is generally used for building structures (in fact, for most non-nuclear structures except bridges). It assures adequate safety against collapse, but as is well known it does not guarantee absence of severe cracking under service conditions. On the other hand, the service stress design is in general more conservative than the limit design, and may require in some cases up to 50% more reinforcement.

In view of its great effect on safety and economy, our choice of the design concept deserves keen attention. Design for the ultimate state rather than the service state is certainly more reasonable from the viewpoint of safety against collapse, but the question as to what is the ultimate state is rather ambiguous. For example, with regard to performance and durability, it would be in many cases most desirable to design for a certain maximum width of cracks in concrete, or for safety against the coalescence of densely distributed hairline cracks into isolated large cracks. However, the necessary mechanics theory is rather complicated and not even satisfactorily understood at present.

The purpose of this paper is to show that there nevertheless exists one, rather realistic, alternative design concept, which is almost as simple as the classical limit design. This concept is also of limit design nature, but, in addition to the yield limit for reinforcement, a friction limit is simultaneously imposed to prevent slip of interlocked rough crack surfaces in concrete. This slip-free limit design eliminates secondary cracking, damage, and disintegration due to breaking the aggregate interlock on the crack surfaces, and generally reduces the extent of cracking. Due to the inelastic volume dilatancy, i.e., volume increase induced by inelastic shear (a phenomenon whose importance for all geological materials has recently been realized), tensile yielding of all steel is caused not merely by the normal displacement but also by the tangential displacement of opposite crack surface. The yield forces in steel not only balance the applied load but also develop compression on the crack surfaces that gives rise to the limit friction force. Consequently, the design against crack slip never leads to a lighter reinforcement than the classical limit design, in which a frictionless slip of crack surfaces is tacitly implied. The reinforcement to assure friction in concrete may be expected to be heavier if the principal tensile forces are inclined with respect to bar directions, for in this case the reinforcing net alone could not carry the load (without concrete).

It must be emphasized that it is not proposed to replace the classical (frictionless) limit design concept, which does provide adequate safety against total collapse. Yet the reduction in cracking and deformation achieved by the slip-free criterion may prove to be desirable in various situations. Adoption of this criterion should

be especially considered for the nuclear vessel and containment codes, as supplementary to the service stress criterion.

In what follows the slip-free criterion for cracks will be analyzed under the following standard assumptions: (1) Concrete has no tensile strength; (2) the bars carry only forces along their axes, i.e., bar kinking, dowel forces, and dowel splitting are neglected (13,16,19,20); and (3) the bars are sufficiently densely distributed and the internal forces are approximately uniform over the distance of several bar spacings. Consideration will be limited to cases where at least one principal internal force is tensile and suffices to produce continuous cracks. Reversed and cyclic loading will not be specifically considered.

**CRACK SLIP CRITERION**

While steel reinforcement yields at strains of about 0.0014 to 0.0025, a far smaller tensile strain, about 0.0001, is sufficient to produce hairline cracks in concrete. These cracks, or other preexisting cracks, gradually open at increasing load and, except when they are precisely normal to the principal stress, they are also subjected to shear, which causes the opposite crack surfaces to displace tangentially. These surfaces are, however, rough. So, after a small tangential displacement the opposite surfaces interlock, even though they may have already moved apart in the normal direction. During subsequent tangential displacement the wedging effect of surface asperities in contact causes further relative normal displacement, which is overall manifested by volume increase due to shear (dilatancy), a phenomenon whose existence has been well documented. The dilatancy is opposed by tension in the reinforcement, which in turn induces in concrete a compressive force that is transmitted across the opened rough crack by means of interlocked asperities.

Limit analysis is applicable only to deformations that occur at roughly constant load (ductile behavior). Whether or not the crack surface friction is to be included in the limit analysis depends on the magnitude that the tangential displacement can reach before friction is lost. Friction is to be taken into account if the overall shear strain of concrete involving frictional sliding of the cracks is much larger than the elastic part of the overall shear strain. In the subsequent section it will be shown by crude calculations that this must indeed be the case. Even from the simple fact that the height of humps (asperities) on the crack surface is at least 5 mm, one can see that the normal surface separation would have to reach at least 5 mm to allow large tangential displacements at zero friction. So the only case where friction could be negligible is when the tangential displacement is much smaller than the normal displacement of crack surfaces. In this case, however, the slip-free and classical criteria given essentially the same result, as shown in the sequel.

Furthermore, it is necessary to show that the dilatancy due to crack slip is large enough to cause tensile yielding in all reinforcement even if the applied load component that is normal to the crack would alone be too small for achieving it. Again, the analysis that follows indicates this to be true or almost true. Furthermore, the volume dilatancy due to inelastic shear of concrete is known to generally exceed 0.002, usually by far, and this is clearly enough to cause tensile yielding of all reinforcement.

By imposing a condition of no slip, one tries to avoid the consequences

of the crack slip. These include crushing and breakage of asperities (surface humps, aggregate pieces) at their roots, spreading of secondary cracks from the original crack, and dowel splitting, which can lead to substantial damage to concrete. Moreover, while before slip the rough crack surfaces are undamaged and would mutually fit upon unloading, the crushed asperities at the surface of a slipped crack prevent full crack closure upon unloading. Thus, crack slip causes deformation irreversibility, which is a manifestation of damage. Sometimes, material and geometrical friction have been distinguished, but the distinction is not precise and we will avoid it.

Let  $N_\theta$  be the component of the applied force resultant normal to the crack of inclination  $\theta$  and let  $N_\theta^s$  be the normal component of the resultant of the limit (yield) axial forces in the reinforcement,  $N_x^s$  and  $N_y^s$  [Fig. 1(d)]. Since a sufficiently large crack slip would always produce sufficient dilatancy, as justified before, the yield forces are certain to be developed in the reinforcement

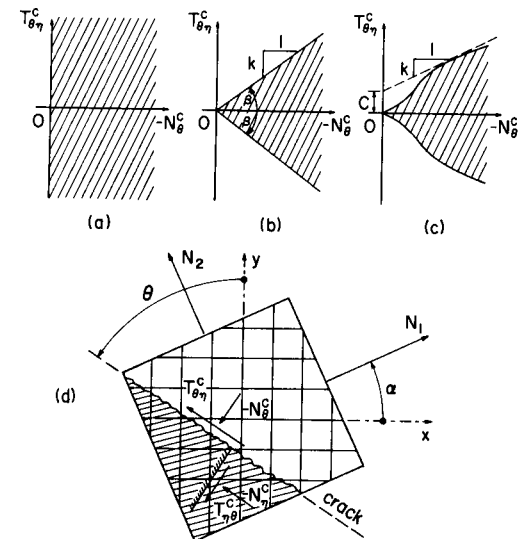


**FIG. 1.—(a) Frictionless Criterion; (b) Proposed Slip-Free Criterion; (c) Slip-Free Criterion with Variable Friction; (d) Internal Forces**

at large enough crack slip, even if the applied normal force component  $N_\theta$  is small.

The condition of no-slip crack surfaces may be written in the form of Coulomb friction criterion:  $kN_\theta^c < T_{\theta\eta}^c < -kN_\theta^c$ , i.e. [Fig. 1(b)]:

$$-k(N_\theta^s - N_\theta) < T_{\theta\eta} - T_{\theta\eta}^s < k(N_\theta^s - N_\theta) \dots \dots \dots (1)$$

in which  $k$  = friction coefficient for the crack surfaces;  $T_{\theta\eta}$  and  $T_{\theta\eta}^s$  = tangential components of the resultants of the applied internal ultimate design forces (due to design loads times proper load factors  $\mu$ ) and of the yield forces in the reinforcement (assumed to be already reduced by the capacity reduction factor  $\phi = 0.9$ );  $T_{\theta\eta} - T_{\theta\eta}^s = T_{\theta\eta}^c$  = shear force carried by concrete; and  $N_\theta - N_\theta^s = N_\theta^c$  = normal force applied on concrete in the crack (Fig. 1).

The friction coefficient,  $k$ , no doubt depends on the crack opening displacement and the shear slip displacement. However, the precise dependence is not well known, and thus  $k$  will be treated as a constant. Paulay and Loeber (22) recommend  $k = 1.7$  and ACI-318 (3) indicates  $k = 1.4$ . However, at a later stage of failure, when concrete between the cracks is partly broken up by secondary cracks and dowel splitting,  $k$  can be less. To be on the safe side, we will consider  $k = 0.75$ , which is about equal to the largest friction coefficient displayed by granular materials. For further information on friction of concrete, see Refs. 12, 17, 18, and 25.

Note that Eq. 1 does not permit existence of any shear force when  $N_\theta^c = N_\theta - N_\theta^s = 0$ . Conversely, if a shear force is present,  $N_\theta^s$  must exceed  $N_\theta$ , while in the usual frictionless design  $N_\theta^s$  may equal  $N_\theta$ . In other words, for the slip-free limit design, the reinforcement must not only balance the applied load but it must also produce enough compression in concrete to develop the friction force that must accompany the sliding. Therefore, the slip-free criterion in Eq. 1 never yields less reinforcement than the classical criterion.

The classical (frictionless) design criterion (1,2,10)

$$N_\theta < N_\theta^s \dots \dots \dots (2)$$

may formally be obtained from Eq. 1 by dividing it by  $k$  and letting  $k \rightarrow \infty$ . It must be realized, however, that for the limit state  $N_\theta = N_\theta^s$  corresponding to  $k = \infty$  there is actually no friction force because  $N_\theta^c = 0$ , whence the term "frictionless."

The idea that the design of reinforcement ought to include in some way an analysis of shear on crack surfaces due to aggregate interlock has occurred before. For example, Baumann (1), using a strain energy approach, considered the implications of compatibility conditions in case of shear displacement on the crack.

However, the role of inelastic dilatancy stemming from crack surface sliding, and the consequent possibility of using a frictional condition in a limit design approach, seem to have eluded attention thus far. Neither has it been realized, it seems, that inclusion of friction in the limit analysis would yield a safer, rather than less safe, design.

**EQUILIBRIUM RELATIONS**

Assume an orthogonal net of reinforcing bars in directions  $x$  and  $y$  [Fig. 1(d)]. Denote by  $N_1$  and  $N_2$  the principal internal forces, such that  $N_1 \geq N_2$ ,  $N_1 > 0$ , and let  $\alpha$  be the angular deviation of force  $N_1$  from axis  $x$ , and  $\theta$  the angular deviation of crack plane from axis  $y$  [both positive if counterclockwise, Fig. 1(d)]. Without loss of generality we can assume that  $0 \leq \alpha \leq \pi/4$  and  $0 \leq \theta \leq \pi$ .

The normal and tangential components of the applied forces  $N_1$ ,  $N_2$  and of the reinforcement yield forces  $N_x^s$ ,  $N_y^s$  on the crack surface, and the normal forces parallel to crack surfaces, are

$$\begin{aligned} N_\theta &= N_1 \cos^2(\theta - \alpha) + N_2 \sin^2(\theta - \alpha); & N_\theta^s &= N_x^s \cos^2 \theta + N_y^s \sin^2 \theta; \\ N_\eta &= N_1 \sin^2(\theta - \alpha) + N_2 \cos^2(\theta - \alpha); & N_\eta^s &= N_x^s \sin^2 \theta + N_y^s \cos^2 \theta; \\ T_{\theta\eta} &= \frac{1}{2}(N_1 - N_2) \sin 2(\theta - \alpha); & T_{\theta\eta}^s &= \frac{1}{2}(N_x^s - N_y^s) \sin 2\theta \dots \dots \dots (3) \end{aligned}$$

Substituting into inequalities in Eq. 1, we obtain

$$g(\theta) = [k(1 + \cos 2\theta) \pm \sin 2\theta] n_x + [k(1 - \cos 2\theta) \mp \sin 2\theta] n_y - k(1 + m) - (1 - m)[k \cos 2(\theta - \alpha) \pm \sin 2(\theta - \alpha)] \geq 0 \dots \dots \dots (4)$$

in which  $n_x = \frac{N_x^s}{N_1}$ ;  $n_y = \frac{N_y^s}{N_1}$ ;  $m = \frac{N_2}{N_1} \dots \dots \dots (5)$

are the ratios of internal forces to  $N_1$ . Without loss of generality we may assume  $m \leq 1$ . For a chosen crack direction  $\theta$  (and given internal forces), Eq. 4 represents a set of two linear inequalities which restrict the reinforcement

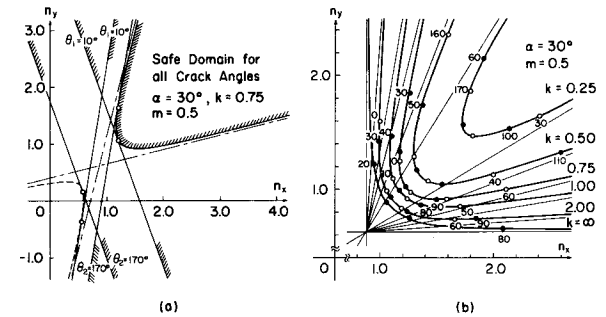


**FIG. 2.—(a) Safe Half Planes for Various Crack Angles and Envelope with Domain Safe for all Crack Angles; (b) Hyperbolic Safe Design Domains for Various Friction Coefficients (Numbers Marked on Envelopes Are Crack Angles)**

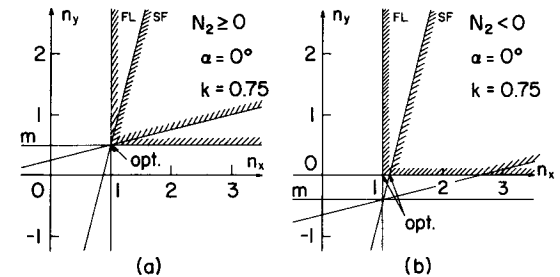


**FIG. 3.—Special Cases of Safe Design Domains for Principal Forces Parallel to Bars**

parameters,  $n_x$  and  $n_y$ , to lie in one of two half planes in the  $(n_x, n_y)$  plane [see Fig. 2(a)]. Such half-plane restrictions are obtained for each crack direction  $\theta$ .

**SAFE DESIGN OF REINFORCEMENT**

A safe design  $(n_x, n_y)$  is a design that satisfies the inequalities for all angles  $\theta$ . So, it must lie within the envelope of all half planes. The equation of the envelope is obtained from the conditions  $g(\theta) = 0$  and  $dg(\theta)/d\theta = 0$ , which

represent two linear equations for  $n_x, n_y$ . Noting that  $1 + k^2 = \sec^2 \beta$  and  $k \cos 2\theta \pm \sin 2\theta = \pm \sec \beta \sin (2\theta \pm \beta)$ , we obtain the solution

$$n_x = 1 - \frac{1}{2} (1 - m) \sin 2\alpha \left[ \frac{\pm \operatorname{cosec} \beta - \sin (2\theta \pm \beta)}{\cos (2\theta \pm \beta)} + \tan \alpha \right] \dots \dots \dots (6)$$

$$n_y = m - \frac{1}{2} (1 - m) \sin 2\alpha \left[ \frac{\pm \operatorname{cosec} \beta + \sin (2\theta \pm \beta)}{\cos (2\theta \pm \beta)} - \tan \alpha \right] \dots \dots \dots (7)$$

in which  $\beta = \arctan (k) =$  friction angle; and  $k$  is the friction coefficient.

Eqs. 6 and 7 represent the parametric equations of the envelope of the safe domain of reinforcement parameters,  $n_x$  and  $n_y$  [see Fig. 2(b)]. Each point of the envelope is associated with a particular crack direction,  $\theta$  [some values of  $\theta$  are marked on the envelope in Fig. 2(b)]. Tracing the sign of the inequality in Eq. 4 up to Eqs. 6 and 7, one can determine that the safe design domain is the cross-hatched one in Fig. 2(a).

Eliminating  $\theta$  from Eqs. 6 and 7, we obtain a single equation for the envelope:

$$\begin{aligned} & [(n_x - n_x^0) - \beta_1 (n_y - n_y^0)] [(n_y - n_y^0) - \beta_1 (n_x - n_x^0)] \\ & = [\beta_2 (1 - m) \sin 2\alpha]^2 \dots \dots \dots (8) \end{aligned}$$

in which  $n_x^0 = \frac{1}{2} (1 + m) + \frac{1}{2} (1 - m) \cos 2\alpha;$

$$\begin{aligned} n_y^0 &= \frac{1}{2} (1 + m) - \frac{1}{2} (1 - m) \cos 2\alpha; \quad \beta_1 = \frac{1 - \sin \beta}{1 + \sin \beta} \\ &= \left[ \tan \left( \frac{\pi}{4} - \frac{\beta}{2} \right) \right]^2; \quad \beta_2 = \frac{1}{1 + \sin \beta} = \left[ 2 \cos \left( \frac{\pi}{4} - \frac{\beta}{2} \right) \right]^{-2} \dots \dots \dots (9) \end{aligned}$$

Eq. 8, which may be verified by substituting Eqs. 6 and 7, is quadratic in  $n_x$  and  $n_y$ , and represents a hyperbola (see Fig. 2). Only one of its two branches applies. Its asymptotes are obtained by setting equal to zero one or the other brackets at the left-hand side of Eq. 8, i.e., the asymptotes are  $n_y = \beta_1^{-1} (n_x - n_x^0) + n_y^0$  and  $n_y = \beta_1 (n_x - n_x^0) + n_y^0$ . They pass through the center  $(n_x^0, n_y^0)$  and have slopes  $\beta_1$  and  $1/\beta_1$  depending (through  $\beta$ ) on the friction coefficient,  $k$ , and on the ratio of applied principal forces,  $m$ . The location of the apex also depends on these variables. The higher is  $k$ , the greater is the angle of the asymptotes, and the closer is the apex to the center. For  $k \rightarrow \infty$  (frictionless criterion), the asymptotes become orthogonal, which coincides with the existing approach (10). The center of the hyperbola is at equal distances from axes  $n_x$  and  $n_y$  if either  $N_1$  and  $N_2$  form angles  $\alpha = 45^\circ$  with the bars or if  $N_1 = N_2$ . The more  $\alpha$  differs from  $45^\circ$ , or the more  $N_2/N_1$  differs from 1, the more unequal these distances become. For  $\alpha = 0$  ( $N_1$  and  $N_2$  being parallel to the bars) and  $m = 0$ , the center of the hyperbola lies on axis  $n_x$ . The proximity of the apex of the hyperbola to its center depends on the right-hand side of Eq. 8; the apex moves closer as the friction coefficient becomes larger, and as the orientation,  $\alpha$ , of  $N_1$  and  $N_2$  turns closer to the bar directions; for  $\alpha = 0$  the hyperbola degenerates into two straight lines that yield a corner domain (see Fig. 3). The same happens when  $N_2/N_1$  approaches 1.

One basic property to note is that the safe domain for any finite friction coefficient lies entirely within the safe domain for  $k \rightarrow \infty$ , i.e., for the classical frictionless criterion. Thus, the slip-free criterion never results in less steel than the frictionless criterion.

The compressive forces that act in concrete in the directions normal and parallel to the crack are  $N_\theta^c = N_\theta - N_\theta^s$  and  $N_\theta^c = N_\theta - N_\theta^s$ , and the shear force transmitted by the crack is  $T_{\theta\eta}^c = T_{\theta\eta} - T_{\theta\eta}^s$ . Substituting from Eq. 3, we obtain

$$\frac{N_\theta^c}{N_1} = \pm \frac{1}{2} (1 - m) \sin 2\alpha \frac{\operatorname{cosec} \beta - \sin \beta}{\cos (2\theta \pm \beta)} \dots \dots \dots (10)$$

$$\frac{N_\eta^c}{N_1} = \pm \frac{1}{2} (1 - m) \sin 2\alpha \frac{\operatorname{cosec} \beta + \sin \beta}{\cos (2\theta \pm \beta)} \dots \dots \dots (11)$$

$$\frac{T_{\theta\eta}^c}{N_1} = - \frac{1}{2} (1 - m) \sin 2\alpha \frac{\cos \beta}{\cos (2\theta \pm \beta)} \dots \dots \dots (12)$$

From  $N_\eta^c$  (and eventually also  $N_\theta^c$  and  $T_{\theta\eta}^c$ ), the minimum necessary thickness,  $h$  (or minimum strength), of concrete can be readily ascertained.

Note that all forces in concrete vanish if  $m = 1$  ( $N_2 = N_1$ ) or  $\alpha = 0$  (principal forces parallel to the bars), provided that  $N_2 \geq 0$  ( $m \geq 0$ ).

The ordinary (frictionless) criterion (Eq. 2) is based on balancing solely the normal force component on the crack, the tangential component being ignored. Fortunately, it appears that if the normal component is balanced for all crack angles  $\theta$  between 0 and  $\pi$ , it is automatically guaranteed that the tangential component of the loading is safely resisted by the yield forces on cracks of all directions (as pointed out to the writers by A. Gupta). This can be verified either by using Eqs. 10-12 or simply by noting that the tangential forces must be balanced for  $k \rightarrow \infty$  since the condition in Eq. 1 guarantees them to be balanced for any  $k$ .

**OPTIMUM SAFE DESIGN OF REINFORCEMENT**

In the absence of other constraints, the optimum design may be simply considered to be the reinforcement of minimum weight. This requires that  $N_x^s + N_y^s = \min$  or  $n_x + n_y = \min$ . Denoting  $f(\theta) = n_x + n_y$ , we may calculate from Eqs. 6 and 7 that  $df(\theta)/d\theta = \pm 2 (1 - m) \sin 2\alpha \operatorname{cosec} \beta \tan (2\theta \pm \beta) / \cos (2\theta \pm \beta)$ . The crack inclination corresponding to the optimum design is then obtained by setting  $df(\theta)/d\theta = 0$ , which provides

$$\theta_{opt} = \frac{\pi}{4} \pm \left( \frac{\pi}{4} - \frac{\beta}{2} \right) \dots \dots \dots (13)$$

Substituting  $\theta = \theta_{opt}$  into Eqs. 6 and 7, we finally obtain the optimum reinforcement parameters

$$(n_x)_{opt} = 1 + \frac{1}{2} (1 - m) \sin 2\alpha (\operatorname{cosec} \beta - \tan \alpha) \dots \dots \dots (14)$$

$$(n_y)_{opt} = m + \frac{1}{2} (1 - m) \sin 2\alpha (\operatorname{cosec} \beta + \tan \alpha) \dots \dots \dots (15)$$

The normal forces in concrete and the shear force transmitted through the crack surface are obtained, for the optimum reinforcement, by substituting  $\theta_{opt}$  in Eqs. 10-12:

$$\left(\frac{N_{\theta}^c}{N_1}\right)_{opt} = -\frac{1}{2}(1-m)\sin 2\alpha(\operatorname{cosec}\beta - \sin\beta) \dots \dots \dots (16)$$

$$\left(\frac{N_{\eta}^c}{N_1}\right)_{opt} = -\frac{1}{2}(1-m)\sin 2\alpha(\operatorname{cosec}\beta + \sin\beta) \dots \dots \dots (17)$$

$$\left(\frac{T_{\theta\eta}^c}{N_1}\right)_{opt} = \pm\frac{1}{2}(1-m)\sin 2\alpha\cos\beta \dots \dots \dots (18)$$

The shear force vanishes for  $\beta = \pi/2$  (i.e.,  $k = \infty$ , the frictionless case),  $\alpha = 0$ , or  $N_2 = N_1$ . Note also that  $(N_{\theta}^c)_{opt} \leq 0$ ; thus, the present slip-free

**TABLE 1.—Percentage Increase  $R$  in Optimum Reinforcement Weight When Replacing Frictionless Design FL by Slip-Free Design SF with  $k = 0.75$**

$\alpha$ , in de- grees	$m$								
	1.00	0.75	0.50	0.25	0.00	-0.25	-0.50	-0.75	-1.00
0	0.0	0.0	0.0	0.0	0.0	<u>6.3</u>	<u>12.5</u>	<u>18.8</u>	<u>25.0</u>
5	0.0	1.7	4.5	6.5	10.3	<u>9.8</u>	<u>14.4</u>	<u>20.2</u>	<u>26.3</u>
10	0.0	2.7	7.2	11.3	17.2	<u>23.7</u>	<u>23.6</u>	<u>26.1</u>	<u>31.2</u>
20	0.0	5.8	12.1	18.5	26.2	<u>34.8</u>	<u>44.5</u>	<u>54.7</u>	<u>66.7</u>
30	0.0	7.1	15.0	22.6	30.5	<u>39.3</u>	<u>48.3</u>	<u>57.1</u>	<u>66.7</u>
45	0.0	8.5	16.5	25.0	33.5	<u>41.5</u>	<u>50.0</u>	<u>58.5</u>	<u>66.7</u>

Note:  $R = [F(0.75)/F(\infty)] \times 100\%$ ;  $F(k) = (n_x + n_y)_{opt} = 1 + m + (1 - m)\sin 2\alpha/\sin\beta$  for  $(n_y)_{opt} \geq 0$ ;  $F(k) = n_x(\theta_0)$  for  $(n_y)_{opt} < 0$  (underlined numbers);  $\beta = \arctan(k)$ .

criterion always gives greater safety margin than the classical frictionless criterion (see Table 1).

While for the frictionless criterion the optimum design is always obtained by considering a crack of  $\theta_{opt} = 45^\circ$ , for the present slip-free criterion the value of  $\theta_{opt}$  strongly depends on the friction coefficient and greatly differs from  $45^\circ$ . For  $k = 0.75$ , we have  $\theta_{opt} = 18.4^\circ$  or  $71.6^\circ$ .

In this context it is interesting to recall the approach of Flügge (8), an early suggestion in which no optimum crack direction was searched and hairline cracks were assumed to form perpendicularly to the reinforcing bars,  $\theta = 0^\circ$  or  $90^\circ$ . It may now be recognized that such cracks are in fact the optimum slip-free cracks if the friction coefficient  $k$  approaches 0. This would certainly be an unreasonably conservative assumption.

Since  $\theta_{opt}$  is independent of the cross-sectional areas of reinforcement and the thickness of concrete, same as in the frictionless criterion (2), the optimum design formulas, Eqs. 14-18, can be obtained quite simply and directly by writing the equilibrium conditions for the crack of proper direction.

Note again that for the frictionless criterion,  $k \rightarrow \infty$ , one has  $\sin\beta = 1$ , which gives the well-known result (1,2,10).

The slip-free condition and the classical condition give the same optimum design if  $m = 1$  ( $N_1 = N_2$ ), or if  $\alpha = 0$  (principal forces are parallel to the bars) [see Fig. 3(a)]. The case  $m = 1$  is a special case of  $\alpha = 0$ . When  $N_2$  is close to  $N_1$ , or when  $\alpha$  is close to zero, the difference in the optimum design according to these two criteria is small. Excluding compression, we obtain the largest difference when  $m = 0$  ( $N_2 = 0$ ) and  $\alpha = 45^\circ$ .

**COMPRESSION IN ONE PRINCIPAL DIRECTION**

The previous results make sense only as long as  $(n_x)_{opt} \geq 0$  and  $(n_y)_{opt} \geq 0$ . It can be verified that the first condition always holds true if  $m \leq 1$ , as assumed at the outset. According to Eq. 15, the second condition can be shown to be equivalent to

$$m \geq \cot(\alpha - \beta_0)\tan\alpha \quad \text{for } \alpha < \beta_0 \dots \dots \dots (19)$$

in which  $\beta_0 = \arctan(k/\sqrt{1+k^2}) = \arctan(\sin\beta)$ . For  $\alpha \geq \beta_0$ ,  $(n_y)_{opt}$  is always non-negative.

If Eq. 19 is violated, Eq. 15 gives  $n_y < 0$ . We must then set  $n_y = 0$  in Eq. 7, which yields

$$\frac{\pm\operatorname{cosec}\beta + \sin(2\theta \pm \beta)}{\cos(2\theta \pm \beta)} = \frac{\tan\alpha + m\cot\alpha}{1-m} \dots \dots \dots (20)$$

The solution of Eq. 20 is the angle  $\theta = \theta_0$  which gives  $n_y = 0$  or  $N_y^s = 0$ . The optimum design is then obtained by substituting  $\theta = \theta_0$  in Eq. 6 in order to get  $n_x$  and  $N_x^s$ , and in Eqs. 10, 11, and 12 in order to get the normal and shear resultants in concrete,  $N_{\theta}^c$ ,  $N_{\eta}^c$ ,  $T_{\theta\eta}^c$ . From these three values, one can determine the principal compression force in concrete that gives the minimum required thickness of concrete,  $h_{min}$ . Note that, for other angles  $\theta \neq \theta_0$ , one would get higher compression forces in concrete, but this is irrelevant because slip on such cracks does not take place, for they are not the critical crack angles. However, one must also check the minimum concrete thickness required to carry  $N_2$  when there is no crack.

The optimum design point in case of compression is shown in Fig. 4. Note that it does not necessarily lie at the apex of the hyperbola, as is the case in Fig. 4(b).

The slip-free and frictionless limit design concepts have been found to give identical results if  $\alpha = 0$  and  $N_2 \geq 0$  [Fig. 3(a)]. This is not the case, however, if  $N_2 < 0$  [Fig. 3(b)].

The cases of compression in both principal directions or a large compression in one direction will not be considered because the limit capacity then depends mainly on nonlinear triaxial response of concrete rather than on reinforcement.

**LOAD CAPACITY OF GIVEN REINFORCEMENT (YIELD CRITERION)**

So far we have considered the optimum design of reinforcement to carry given internal forces. This is the inverse of the more basic problem of load capacity of a slab of given thickness and given reinforcement.

Assuming that all reinforcement yields and the crack surfaces slip, we in effect imply the existence of a failure mechanism. The equations of equilibrium on the crack (Eqs. 1 and 3 with equality signs) are equivalent to virtual work equations for the failure mechanism represented by a slip on the crack. So, our approach is that of the *upper bound* theorem of limit analysis, and not the lower bound theorem as some authors incorrectly stated, being misled by the term "principle of minimum resistance," which is an unnecessary deviation from limit analysis terminology. (In a lower bound approach one would have to consider all admissible equilibrium states that are at or below the yield or slip point, including all states where only one of the two systems of bars yields and the friction is equal to or less than the limit value.)

The load multiplier,  $\mu$ , is proportional to  $N_1$ ; therefore  $\mu \sim N_1/N_x^s$  where the yield force  $N_x^s$  is fixed. Obviously,  $\mu \sim 1/n_x$ . Since  $N_y^s$  is also fixed, the ratio  $n_x/n_y$  is constant. According to the upper bound theorem, one must find the critical crack direction,  $\theta_{cr}$ , that gives the smallest load multiplier,  $\mu$ , i.e., the largest  $n_x$  at fixed reinforcement. Writing the equilibrium equation in Eq. 4 in the form  $An_x + Bn_y + C = 0$  with  $n_y = (n_y/n_x)n_x$ , differentiating with respect to  $\theta$ , and setting  $dn_x/d\theta = 0$ , we obtain  $(\partial A/\partial\theta)n_x + (\partial B/\partial\theta)n_y$

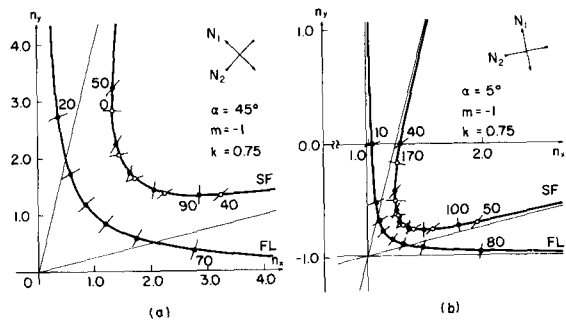


FIG. 4.—Examples of Safe Design Domains

$+ \partial C/\partial\theta = 0$  for  $\theta = \theta_{cr}$ . By comparison with Eq. 4 we see that this is equivalent to the condition  $dg(\theta)/d\theta = 0$  which was used to obtain the envelope.

Consequently, the angle  $\theta$  that ensues from Eqs. 6 and 7 [marked on the envelope in Fig. 2(b)] is the critical crack angle,  $\theta_{cr}$ , which gives the lowest upper bound load multiplier and represents the true direction of the major crack that forms during the failure process in accordance with our starting assumptions.

It is instructive to express the yield surface,  $F(N_x, N_y, N_{xy}) = 0$ . Noting that  $n_x^0 = N_x/N_1$ ,  $n_y^0 = N_y/N_1$ ,  $n_x = N_x^s/N_1$ ,  $n_y = N_y^s/N_1$ , and  $(1 - m) \sin 2\alpha = 2N_{xy}/N_1$ , we obtain from Eq. 8 the yield condition:

$$F = [(N_x^s - N_x) - \beta_1(N_y^s - N_y)] [(N_y^s - N_y) - \beta_1(N_x^s - N_x)] - (2\beta_2 N_{xy})^2 = 0 \dots \dots \dots (21)$$

Note that for  $k \rightarrow \infty$  it reduces to the well-known form  $(N_x^s - N_x)(N_y^s - N_y) = N_{xy}^2$  (10). For illustration, the yield surface according to Eq. 21 is plotted in Fig. 5.

EQUIVALENCE OF OPTIMUM SERVICE STRESS AND LIMIT FRICTIONLESS DESIGNS

The service stress concept was presented (6) as a method of evaluating a given design. It is, however, easy to determine from the formulation in Ref. 6 the conditions of optimum design (lowest weight of steel). Appendix I shows that the optimum is obtained if the reinforcements of both directions reach their allowable stress simultaneously, i.e., the strains of both equal the strain at the onset of yield divided by the same safety factor. Then, however, the equilibrium conditions on the crack are identical to those for the limit frictionless design (but for a common multiplier). This leads us to an interesting conclusion, which seems to have passed unnoticed so far, i.e., the optimum frictionless design is actually *equivalent* to the optimum service stress design except for a common scaling factor. (This is of course not true for designs that are not

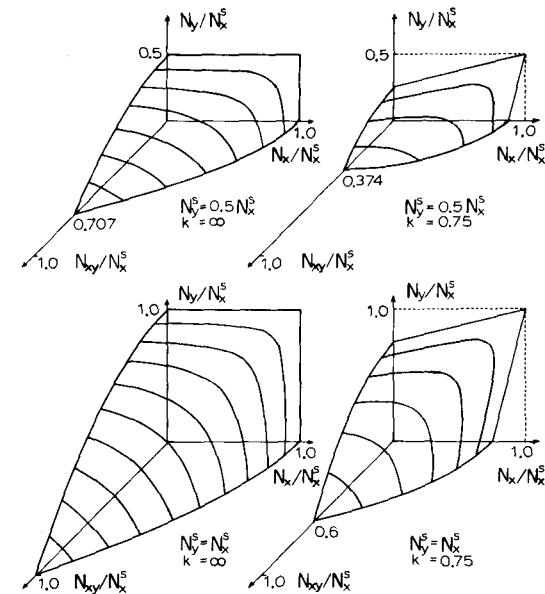


FIG. 5.—Yield Surface for Frictionless Criterion ( $k \rightarrow \infty$ ) and Proposed Slip-Free Criterion ( $k = 0.75$ ) (Contour Lines Are at Intervals of 0.1)

optimum in the sense of the weight of steel.)

The foregoing conclusion may be regarded as *fundamentally objectionable*; the failure process is different from the service behavior, and so the design concepts must be also different (just as is the case with the limit design of continuous beams, frames, slabs, or shells). It is therefore also illogical that the allowable stresses give different optimum reinforcements. For structures where the failure state approach is acceptable (non-nuclear structures), the allowable stresses for the design of reinforcing nets should logically be specified so that the resulting design be identical, in case that the frictionless failure criterion is deemed to be appropriate.

## NUMERICAL EXAMPLES

To demonstrate typical differences between various design concepts, four different examples defined in Table 2 (all for  $k = 0.75$ ) have been calculated according to the preceding equations. For comparisons with the service stress design (6), further data must be given, i.e., the ratio of dead to live load must be specified (see Table 2) and the respective load factors are taken as 1.4 and 1.7. The yield stress of reinforcement is taken as  $f_y = 276 \text{ MN/m}^2$ , and applying the capacity reduction factor  $\phi = 0.9$ , this is reduced to  $248.4 \text{ MN/m}^2$ . The strength of concrete is considered as  $f'_c = 4,000 \text{ psi}$  ( $27.56 \text{ MN/m}^2$ ), and the ultimate stress in concrete for determining the minimum concrete thickness is taken as  $\phi(0.85 f'_c)$  with  $\phi = 0.9$ . The allowable stress of concrete is taken as  $0.45 f'_c$  and in steel as  $0.5 f_y$ . The elastic moduli of steel ( $E_s = 200,000$

TABLE 2.—Optimum Reinforcement for Various Design Approaches in Typical Examples ( $k = 0.75$ )

Example	1			2			3			4		
	FL	SF	SS									
$N_1$ (kN/m)	400			400			400			400		
$N_2$ (kN/m)	200			0			-400			200		
$\alpha$	$30^\circ$			$45^\circ$			$45^\circ$			$15^\circ$		
h (cm)	10			10			15			10		
Dead-to-live load ratio	3:1			3:1			3:1			1:1		
Design approach*	FL	SF	SS									
Theoretical min. thickness, $h_{\min}$ (cm)	1.21	1.62	1.40	2.80	3.73	3.22	5.60	7.46	6.45	0.74	0.98	0.81
$\theta_{\text{opt}}$	$45.0^\circ$	$71.6^\circ$ $18.4^\circ$	$45.0^\circ$									
$P_x$ (%)	2.59	2.94	3.16	2.37	3.17	2.90	1.58	2.64	1.93	2.73	2.94	3.16
$P_y$ (%)	2.00	2.34	2.44	2.37	3.17	2.90	1.58	2.64	1.93	1.65	1.86	1.91
$P_x + P_y$ (%)	4.59	5.28	5.60	4.75	6.35	5.80	3.17	5.28	3.86	4.38	4.80	5.07
Difference in $P_x + P_y$ from FL (%)	0	15.0	22.0	0	33.3	22.0	0	66.7	22.0	0	9.6	15.8

\*FL = frictionless criterion      SF = slip-free criterion  
SS = service stress design

$\text{MN/m}^2$ ) and concrete ( $E_c = 24,800 \text{ MN/m}^2$ ) used in the calculations are actually irrelevant for the optimum design, as deduced before.

The results of the calculations are given in Table 2. The optimum weights of steel differ up to 67%. The minimum required thickness of concrete,  $h_{\min}$ , falls far below reasonable values, except when the slab is subjected to pure shear parallel to reinforcement (Example 3). The slip-free limit design can give either higher or lower reinforcement than the service stress design, depending on the dead-to-live load ratio and the direction of principal forces. However, if a higher friction coefficient,  $k$ , were considered ( $k = 1.4$ ), the slip-free limit design (SF) would generally come between the frictionless limit design (FL) and the service stress design (SS). As deduced before, the difference between

the service stress and limit frictionless designs is due exclusively to the specified choice of load factors and allowable stresses.

## SHEAR DEFORMATION AND ANALYSIS OF SLIP-FREE CRITERION

The idea of limit design for crack slip is predicated upon the assumption that the load-deformation diagram exhibits a long plateau when the limit load for crack slip is reached. To demonstrate that this is indeed so (except in cases where the frictionless criterion gives identical or rather close results), consider loads  $N_1$  and  $N_2$  at angle  $\alpha = 30^\circ$ , and let them increase in proportion such that  $N_2 = N_1/2$ . The friction coefficient is  $k = 0.75$ , and the reinforcement ratios are assumed as  $p_x = 4.000\%$  and  $p_y = 3.191\%$ , which is in the optimum ratio for the specified data. The yield stress of reinforcement is  $276 \text{ MN/m}^2$ . The concrete slab is 10 cm thick, has a strength of  $27.6 \text{ MN/m}^2$ , an elastic modulus  $E_c = 24,800 \text{ MN/m}^2$ , and an elastic shear modulus  $G_c = 10,500 \text{ MN/m}^2$ . The steel bars have an elastic modulus  $E_s = 200,000 \text{ MN/m}^2$ . Our objective is to estimate the diagram of the shear force,  $T_{\theta_n}$ , on the crack versus the averaged shear strain,  $\bar{\gamma}_{\theta_n}$ , over an area of slab containing many parallel cracks. The mean crack spacing will be assumed as  $a = 5 \text{ cm}$ .

The shear angle is  $\beta = \arctan 0.75 = 36.87^\circ$  and the critical crack angle, according to Eq. 13, is  $\theta_{cr} = 71.57^\circ$  or  $18.43^\circ$ . Let us choose  $71.57^\circ$ . Then  $N_1$  and  $N_2$  form angles  $48.43^\circ$  and  $41.57^\circ$  with the crack. From Eqs. 6 and 7 we obtain that slip of the crack surfaces and yield of all the reinforcement is reached when  $N_1 = 893.2 \text{ kN/m}$ . From Eq. 3, the total applied shear force on the crack surface is  $T_{\theta_n} = 221.7 \text{ kN}$ , and according to Eq. 18 the shear force carried across the crack by aggregate interlock is  $T_{\theta_n}^c = 154.7 \text{ kN/m}$ .

Let us now estimate the shear and normal strains at the point when the slip on the crack as well as the yield of steel is attained. The yield stress in the bars of inclination  $71.57^\circ$  to the crack is reached when the averaged normal strain is about  $\bar{\epsilon}_\theta = \epsilon_y / \sin^2 71.57^\circ \approx 0.0015$  because  $\epsilon_y = f_y / E_s = 276 / 200,000$ . The normal force in concrete is  $N_\theta^c = -T_{\theta_n}^c / k = -206.3 \text{ kN/m}$  and the elastic normal strain of concrete between the cracks is  $\epsilon_\theta^e = -206.3 \text{ kN/m} / (24,800 \text{ MN/m}^2 \times 10 \text{ cm}) = -0.000832$ . So, in order to induce yield of steel the slip on the crack must produce relative to concrete the mean normal strain  $\bar{\epsilon}_\theta = 0.0015 - (-0.000832) = 0.0016$  (the contribution of elastic strain is negligible), this corresponds to crack opening width  $0.0016 \times 5 \text{ cm} = 0.08 \text{ mm}$ . Assuming that the mean slope of surface asperities on the crack is about 1:1, the crack slip to produce opening width 0.08 mm is also about 0.08 mm, which corresponds to the mean shear strain  $\bar{\gamma}_{\theta_n} = 0.08 \text{ mm} / 5 \text{ cm} \approx 0.0016$ . Anyhow, this estimate must be good as far as the order of magnitude goes. [To the  $\bar{\gamma}_{\theta_n}$  value one might add the elastic shear strain due to concrete between the cracks,  $\gamma_{\theta_n}^e = 154.7 \text{ kN/m} / (10 \text{ cm} \times 10500 \text{ MN/m}^2) \approx 0.00016$ ; this is, however, negligible.] To sum up, the yield in steel and the crack slip are reached at  $T_{\theta_n}^c = 154.7 \text{ kN/m}$ ,  $T_{\theta_n} = 221.7 \text{ kN/m}$ ,  $N_\theta^c = -206.3 \text{ kN/m}$ ,  $\bar{\gamma}_{\theta_n} = 0.0016$ , and  $\bar{\epsilon}_\theta = 0.0016$ .

After this state is reached, the reinforcement is yielding and the crack is slipping at roughly constant  $N_1$  and  $N_2$  (assuming that  $k$  is about constant). During this process, the crack width continues to expand (inelastic dilatancy). If the surface asperities on the crack did not break, the maximum expansion

in crack width would equal the height of surface asperities (humps), which is at least half the aggregate size, or about 7 mm. Because of breakage and crushing, the maximum expansion will be less. A safe low guess is about 2 mm. After this maximum expansion is passed, further slip would allow reduction of crack width. This, however, would not occur because the reinforcement yields in tension. So, further slip causes separation of crack surfaces, loss of aggregate interlock, and drop of the frictional force on the crack to zero, which represents the state corresponding to the frictionless criterion.

Knowing that the elastic strains are negligible, the state of the maximum crack width of 2 mm corresponds roughly to  $\bar{\epsilon}_8 = 2 \text{ mm}/5 \text{ cm} = 0.04$  and  $\bar{\gamma}_{\theta_7} = 0.04$ . The associated forces follow from Eqs. 3-7 and 10-12 by substituting  $k \rightarrow \infty$ . Because the reinforcement is not the optimum design for this stage, bars of both directions do not reach yield after the loss of friction simultaneously. From Eq. 6, if the bars of the  $x$  direction yield,  $N_1 = 724.2 \text{ kN/m}$ , and from Eq. 7 if the bars of the  $y$  direction yield,  $N_1 = 1,263 \text{ kN/m}$ . From the latter result,  $T_{\theta_7} = 313.5 \text{ kN/m}$ . These values refer to the crack of angle  $71.57^\circ$ .

The results of these calculations are plotted in Fig. 6. It is noteworthy that the stage of frictional slip on the crack indeed corresponds to a long horizontal plateau, and the frictionless condition develops only after a very large deformation.

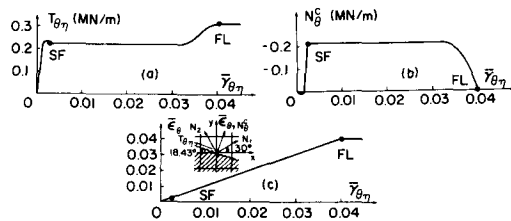


FIG. 6.—Crude Theoretical Estimate of Typical Shear Response Diagram

Therefore, it is quite logical to consider the long first plateau indicated by the slip-free criterion as the basis for limit design.

One crude simplification in the foregoing calculation is that the crack angle has been considered to be the same at all stages of loading. Actually, the first hairline tensile cracks, which are generally discontinuous, appear well before the slip-free limit state; their direction is calculated by the service stress approach using conditions of compatibility (see Ref. 6), which yields crack angle  $44.76^\circ$ . Subsequently, at onset of crack slip, cracks of angle  $71.57^\circ$  should appear. These must be wider and continuous. Finally, for the last stage of friction loss, the critical crack angle follows by substituting  $\beta = \pi/2$  in Eqs. 6 and 7, setting  $n_y/n_x = 0.03191/0.04000$  and solving for  $\theta$ , which yields crack angle  $\theta = 42.86^\circ$ . Thus, at the frictional slip stage, concrete must actually be cracked in two directions (although only one crack system is probably continuous) and at the frictionless slip stage concrete must be cracked in three directions, according to our cracking concept.

The preceding crude analysis indicates, however, the need for a much deeper study of the process of inelastic deformation, crack width and spacing, subsequent formation of crack systems of various directions, shear force transmission on

the cracks, volume expansion due to cracks, and the question of stability of crack systems as well as overall deformation in presence of strain-softening.

POSSIBLE FURTHER EXTENSIONS

**Variable Friction Coefficient and Cohesion.**—After more solid experimental information on aggregate interlock becomes available, it may be worthwhile to consider the dependence of friction coefficient  $k$ , upon normal force  $N_\theta^c$ , which corresponds to a curved envelope of limit states of crack slip [see Fig. 1(c)]. Making a guess of the  $N_\theta^c$  magnitude, this curved envelope may be replaced by the tangent (or secant) straight line [Fig. 1(c)], in which case Eq. 1 is replaced by

$$-C - k(N_\theta^s - N_\theta) < T_{\theta_7} - T_{\theta_7}^s < C + k(N_\theta^s - N_\theta) \dots \dots \dots (22)$$

Here  $C$  is a fictitious cohesion [Fig. 1(c)]. Note that  $k \rightarrow \infty$  again yields the frictionless concept (Eq. 2). The analysis of this case is completely analogous to the previous one (for  $C = 0$ ) and leads to equations of the same form as before, except that  $n_x, n_y, N_\theta^c/N_1, N_\eta^c/N_1$  are replaced by  $n_x - A, n_y - A, (N_\theta^c/N_1) + A, (N_\eta^c/N_1) + A$ , respectively, where  $A = c \cot \beta$  and  $c = C/N_1$ . In particular, Eqs. 6, 7, 9, 10, and 11 are generalized as:

$$\left. \begin{aligned} n_x &= 1 - c \cot \beta - \frac{1}{2} (1 - m) \sin 2\alpha \left[ \frac{\pm \operatorname{cosec} \beta - \sin (2\theta \pm \beta)}{\cos (2\theta \pm \beta)} + \tan \alpha \right] \\ n_y &= m - c \cot \beta - \frac{1}{2} (1 - m) \sin 2\alpha \left[ \frac{\pm \operatorname{cosec} \beta + \sin (2\theta \pm \beta)}{\cos (2\theta \pm \beta)} - \tan \alpha \right] \end{aligned} \right\} \dots \dots \dots (23)$$

$$\left. \begin{aligned} n_x^0 &= \frac{1}{2} (1 + m) - c \cot \beta + \frac{1}{2} (1 - m) \cos 2\alpha \\ n_y^0 &= \frac{1}{2} (1 + m) - c \cot \beta - \frac{1}{2} (1 - m) \cos 2\alpha \end{aligned} \right\} \dots \dots \dots (24)$$

$$\frac{N_\theta^c}{N_1} = c \cot \beta \pm \frac{1}{2} (1 - m) \sin 2\alpha \frac{\operatorname{cosec} \beta - \sin \beta}{\cos (2\theta \pm \beta)} \dots \dots \dots (25)$$

$$\frac{N_\eta^c}{N_1} = c \cot \beta \pm \frac{1}{2} (1 - m) \sin 2\alpha \frac{\operatorname{cosec} \beta + \sin \beta}{\cos (2\theta \pm \beta)} \dots \dots \dots (26)$$

Eqs. 8, 12, 13, and 18 do not change and Eqs. 14, 15, 16, and 17 are generalized as

$$(n_x)_{\text{opt}} = 1 - c \cot \beta + \frac{1}{2} (1 - m) \sin 2\alpha (\operatorname{cosec} \beta - \tan \alpha) \dots \dots \dots (27)$$

$$(n_y)_{\text{opt}} = m - c \cot \beta + \frac{1}{2} (1 - m) \sin 2\alpha (\operatorname{cosec} \beta + \tan \alpha) \dots \dots \dots (28)$$

$$\left( \frac{N_\theta^c}{N_1} \right)_{\text{opt}} = c \cot \beta - \frac{1}{2} (1 - m) \sin 2\alpha (\operatorname{cosec} \beta - \sin \beta) \dots \dots \dots (29)$$

$$\left(\frac{N_c}{N_1}\right)_{opt} = c \cot \beta - \frac{1}{2} (1 - m) \sin 2\alpha (\operatorname{cosec} \beta + \sin \beta) \dots \dots \dots (30)$$

In view of Eq. 23, the safe domain for  $c \neq 0$  is obtained by shifting the envelope given in Eqs. 8 and 9 [e.g., Fig. 2(b)] by the distances  $(-c \cot \beta)$  in both the  $n_x$  and  $n_y$  directions. Thus, the envelope for friction with cohesion lies between those for the frictionless criterion and for the slip-free criterion of the same  $k$ .

**Bending and Multidirectional Nets.**—Extension to bending and twist in shell walls may be easily achieved in the same manner as for the frictionless criterion (1,2,9,11). The principal bending moments are represented by internal force couples and the tensile forces in these couples may be attributed to a layer in the shell, treated like an in-plane loading. This is of course a crude approximation and further research is needed, especially for cases where the signs of the principal moments are opposite.

Extension to skew nets and nets with bars of more than two directions is straightforward and can be done similarly as for the frictionless criterion (1).

**CONCLUSIONS**

1. The proposed slip-free limit design concept assures improved and proper safety against large shear deformations of concrete, thereby reducing the extent of cracking and damage of concrete.
2. The slip-free concept never gives lighter reinforcement than the frictionless limit design concept used so far. The results are the same only if the principal applied internal forces are in the direction of bars and are both tensile. Differences increase with the inclination of principal forces and with the difference between these forces; they reach about 34% for uniaxial tension at a 45° angle with the bars, and about 67% for pure shear along bar directions.
3. The safe design domain envelope is one branch of a hyperbola with nonorthogonal asymptotes.
4. The crack direction giving the lightest possible reinforcement is independent of loading and plate properties. While in the frictionless concept this direction is at 45° to the bars, here the crack angle with the bars equals half the shear angle that applies for slip of crack surfaces.
5. If one principal applied force is compressive, the crack angle for optimum design differs from the foregoing values.
6. Because of volume dilatancy, yield of bars is always induced in all bars by inelastic shear. Before the frictionless limit state is reached, the response diagram for loading that involves shear must exhibit, according to standard analysis assumptions, a long plateau that corresponds to frictional sliding of crack surfaces.
7. The slip-free design is almost as simple to carry out as the frictionless design.
8. Variable friction coefficient may be rather simply treated as constant friction coefficient accompanied by a fictitious cohesion on the crack.
9. The optimum frictionless design used thus far is equivalent to the optimum service stress design (except for a common multiplier). This feature is objectionable.

**Remark.**—Experimental confirmation of the present model would require more sophisticated tests than those already carried out (16,23). The available data give information mostly on the final failure with large cracks, which is the frictionless stage, and scant information exists on prefailure states when the crack opening is not pronounced.

**ACKNOWLEDGMENT**

Support by the National Science Foundation under Grant ENG 75-14848 is gratefully acknowledged. Thanks are due to A. Gupta of IIT Research Institute, Chicago, for many valuable comments and suggestions.

**APPENDIX I.—OPTIMIZATION OF SERVICE STRESS DESIGN**

The normal strains that are normal and parallel to the crack are denoted as  $\epsilon_\theta$  and  $\epsilon_\eta$ . For an orthogonal net, equilibrium requires that

$$p_x \cos^2 \theta \epsilon_\theta + \left(p_x + \frac{1}{n}\right) \sin^2 \theta \epsilon_\eta = \frac{N_x}{A_g E_s};$$

$$p_y \sin^2 \theta \epsilon_\theta + \left(p_y + \frac{1}{n}\right) \cos^2 \theta \epsilon_\eta = \frac{N_y}{A_g E_s}; \quad - \frac{\sin 2\theta}{2n} \epsilon_\eta = \frac{N_{xy}}{A_g E_s} \dots \dots (31)$$

in which  $p_x, p_y$  = reinforcement percentages relative to the gross area of cross section,  $A_g$ ; and  $n = E_s/E_c$ . The optimum reinforcement is obviously obtained by imposing the condition that  $\epsilon_x = \epsilon_y = \epsilon_\gamma$  = strain at onset of yield of steel. Substituting this into the identities:  $\epsilon_\theta = \epsilon_x \cos^2 \theta + \epsilon_y \sin^2 \theta + \epsilon_{xy} \sin 2\theta$ ,  $\epsilon_\eta = \epsilon_x \sin^2 \theta + \epsilon_y \cos^2 \theta - \epsilon_{xy} \sin 2\theta$ , and  $\epsilon_{xy} = (1/2)(\epsilon_\theta - \epsilon_\eta) \sin 2\theta$ , we have  $\epsilon_\theta = \epsilon_\gamma + (1/2)(\epsilon_\theta - \epsilon_\eta) \sin^2 2\theta$ ,  $\epsilon_\eta = \epsilon_\gamma - (1/2)(\epsilon_\theta - \epsilon_\eta) \sin^2 2\theta$ . Thus,  $\epsilon_\theta + \epsilon_\eta = 2\epsilon_\gamma$ ,  $(\epsilon_\theta - \epsilon_\eta) \cos^2 2\theta = 0$ . Considering that  $\epsilon_\theta > 0$  and  $\epsilon_\eta < 0$ , we conclude from the second condition that  $\theta = \pi/4$  for  $N_{xy} > 0$ , or  $3\pi/4$  for  $N_{xy} < 0$ . Thus, we obtain

$$\epsilon_\eta = -2n \frac{|N_{xy}|}{A_g E_s} = - \frac{2|N_{xy}|}{A_g E_c}; \quad \epsilon_\theta = 2\epsilon_\gamma - \epsilon_\eta = 2\epsilon_\gamma + 2n \frac{|N_{xy}|}{A_g E_s} \dots \dots (32)$$

$$\frac{1}{2} p_x \epsilon_\theta - \left(p_x + \frac{1}{n}\right) n \frac{|N_{xy}|}{A_g E_s} = \frac{N_x}{A_g E_s};$$

$$\frac{1}{2} p_y \epsilon_\theta - \left(p_y + \frac{1}{n}\right) n \frac{|N_{xy}|}{A_g E_s} = \frac{N_y}{A_g E_s} \dots \dots \dots (33)$$

Solving for  $p_x$  and  $p_y$ , we acquire  $p_x = (N_x + |N_{xy}|)/(\epsilon_\gamma A_g E_s)$ ,  $p_y = (N_y + |N_{xy}|)/(\epsilon_\gamma A_g E_s)$ . Now, if we use the notations  $N_x^s = (E_s \epsilon_\gamma)(A_g p_x)$  and  $N_y^s = (E_s \epsilon_\gamma)(A_g p_y)$ , we finally obtain  $N_x^s = N_x + |N_{xy}|$  and  $N_y^s = N_y + |N_{xy}|$  which is equivalent to the results given by the frictionless criterion (10).

**APPENDIX II.—REFERENCES**

1. Baumann, T., "Zur Frage der Netzbewehrung von Flächentragwerken," *Der Bauingenieur*, Vol. 47, No. 10, 1972, pp. 367-377.

2. Brondum-Nielsen, T., "Optimum Design of Reinforced Concrete Shells and Slabs," *Report No. R.44*, Structural Research Laboratory, University of Denmark, Copenhagen, Denmark, 1974, pp. 190-200.
3. "Building Code Requirements for Reinforced Concrete," ACI 318-77, ACI Committee 318, American Concrete Institute, Detroit, Mich., 1977.
4. "Code for Concrete Reactor Vessels and Containments," ACI 359-74, ACI-ASME Committee 359, American Concrete Institute, Detroit, Mich., 1974; ASME Boiler and Pressure Vessel Code, Section C13, Concrete Reactor Vessels, American Society of Mechanical Engineers, New York, N.Y., 1974.
5. "Code Requirements for Nuclear Safety Related Concrete Structures," ACI 349-76, ACI Committee 349, American Concrete Institute, Detroit, Mich., 1976.
6. Duchon, N. B., "Analysis of Reinforced Concrete Membrane Subject to Tension and Shear," *American Concrete Institute Journal, Proceedings*, Vol. 69, No. 9, Sept., 1972, pp. 578-583.
7. Falconer, B. H., "Theory of Stresses Induced in Reinforced Concrete by Applied Two-Dimensional Stress," *American Concrete Institute Journal, Proceedings*, Vol. 53, No. 3, Sept., 1956, pp. 277-294.
8. Flüge, W., *Statik und Dynamik der Schalen*, 1st ed., Springer-Verlag, Berlin, Germany, 1934, pp. 13-21.
9. Gambarova, P., and Dei Poli, S., "Influenza delle caratteristiche di armatura sulla fessurazione di piastre di c.a. con armatura a maglia quadrangolare" *Costruzioni in Cemento Armato, Studi e Rendiconti*, Politecnico di Milano, Italcementi, Milan, Italy, 1977, pp. 53-95.
10. Gupta, A. K., "Proposed Addition to Proposed ACI Standard: Code Requirements for Nuclear Safety Related Concrete Structures," *American Concrete Institute Journal, Proceedings*, Vol. 73, No. 7, July, 1976, pp. 431-432.
11. Gupta, A. K., and Sen, S., "Design of Flexural Reinforcement in Concrete Slabs," *Journal of the Structural Division*, ASCE, Vol. 103, No. ST4, Proc. Paper 12888, Apr., 1977, pp. 793-804.
12. Hofbeck, J. A., Ibrahim, I. O., and Mattock, A. H., "Shear Transfer in Reinforced Concrete," *American Concrete Institute Journal, Proceedings*, Vol. 66, No. 2, Feb., 1969, pp. 119-128.
13. Jain, S. C., and Kennedy, J. B., "Yield Criterion for Reinforced Concrete Slabs," *Journal of the Structural Division*, ASCE, Vol. 100, No. ST3, Proc. Paper 10409, Mar., 1974, pp. 631-644.
14. Kuyt, B., "Zur Frage der Netzbewehrung von Flächentragwerken," *Beton und Stahlbetonbau*, Vol. 59, No. 7, 1964, pp. 158-163.
15. Leitz, H., "Eisenbewehrte Platten bei allgemeinem Biegunszustand," *Die Bautechnik*, Vols. 16 and 17, 1923.
16. Lenschow, R., and Sozen, M. A., "A Yield Criterion for Reinforced Concrete Slabs," *American Concrete Institute Journal, Proceedings*, Vol. 64, No. 5, May, 1967, pp. 266-273.
17. Mattock, A. H., "Shear Transfer in Concrete Having Reinforcement at an Angle to the Shear Plane," *Shear in Reinforced Concrete, Special Publication SP-42*, American Concrete Institute, Detroit, Mich., 1974, pp. 17-42.
18. Mattock, A. H., and Hawkins, N. M., "Shear Transfer in Reinforced Concrete—Recent Research," *Journal of the Prestressed Concrete Institute*, Vol. 17, No. 2, Mar./Apr., 1972, pp. 55-75.
19. Morley, C. T., "Experiments on the Distortion of Steel Bars across Cracks in Reinforced Concrete Slabs," *Magazine of Concrete Research*, Vol. 18, No. 54, Mar., 1966, pp. 25-34.
20. Morley, C. T., "Experiments on the Yield Criterion of Isotropic Reinforced Concrete Slabs," *American Concrete Institute Journal, Proceedings*, Vol. 64, No. 1, Jan., 1967, pp. 40-45.
21. Morley, C. T., "Skew Reinforcement of Concrete Slabs against Bending and Torsional Moments," *The Institution of Civil Engineers, Proceedings*, Vol. 42, Jan., 1969, pp. 57-74.
22. Paulay, T., and Loeber, P. J., "Shear Transfer by Aggregate Interlock," *Shear in Reinforced Concrete, Special Publication SP-42*, American Concrete Institute, Detroit, Mich., 1974, pp. 1-15.

23. Peter, J., "Zur Bewehrung von Scheiben und Schalen für Hauptspannungen schiefwinklig zur Bewehrungsrichtung," *Die Bautechnik*, Vol. 43, No. 5, 1966, pp. 149-154; Vol. 43, No. 7, 1966, pp. 240-248.
24. Sholz, G., "Zur Frage der Netzbewehrung von Flächentragwerken," *Beton und Stahlbetonbau*, Vol. 53, No. 10, 1958, pp. 250-255.
25. Taylor, H. P. J., "The Fundamental Behavior of Reinforced Concrete Beams in Bending and Shear," *Shear in Reinforced Concrete, Special Publication SP-42*, American Concrete Institute, Detroit, Mich., 1974, pp. 43-77.

#### 14344 REINFORCED NET: OPTIMUM SLIP-FREE DESIGN

**KEY WORDS:** Concrete; Concrete (prestressed); Concrete (reinforced); Concrete slabs; Ductility; Failure; Friction; Inelastic action; Limit analysis; Limit design; Optimum design; Plasticity; Reinforcement; Shells

**ABSTRACT:** The proposed slip-free design assures desired safety against large frictional shear slip of crack surfaces, which assures a reduced extent of cracking and damage to concrete. Orthogonal nets in shell or plate walls under in-plane forces are considered. A reinforcement that is up to about 34% heavier is obtained when large shear forces in the bar directions are present. The case when one principal force is compressive is also analyzed, and here the differences become still larger (up to about 67%). The optimum classical (frictionless) limit design is found to be equivalent to the optimum service stress design (except for a common scaling factor), which is an objectionable feature, and the difference between them is due solely to safety factors. In the slip-free design, which is almost as simple as the frictionless design, the critical crack direction leading to the lightest possible reinforcement is not at a 45° angle with the bars, as in the frictionless design, but deviates from it substantially. The safe domain in the plane whose coordinates are the reinforcement ratios is still a hyperbola, but with inclined asymptotes.

**REFERENCE:** Bazant, Zdenek P., and Tsubaki, Tatsuya, "Concrete Reinforcing Net: Optimum Slip-Free Limit Design," *Journal of the Structural Division*, ASCE, Vol. 105, No. ST2, **Proc. Paper 14344**, February, 1979, pp. 327-346